Supporting Information for

Graphene Foam: Uniaxial Tension Behavior and Fracture Mode Based on a Mesoscopic Model

Douxing Pan,[†,‡,§,#] Chao Wang,[†,‡,#] Tzu-Chiang Wang,[†,‡,*] and Yugui Yao[†,*]

[†]Beijing Key Laboratory of Nanophotonics and Ultrafine Optoelectronic Systems, School of Physics, Beijing Institute of Technology, Beijing 100081, China

[‡]The state key laboratory of nonlinear mechanics, Institute of Mechanics, Chinese Academy of Sciences, Beijing 100190, China

[§]School of Engineering Science, University of Chinese Academy of Sciences, Beijing 100049, China

[#]These two authors contributed to the work equally.

*Corresponding authors: tcwang@imech.ac.cn (TCW); ygyao@bit.edu.cn(YGY)

PREMBLE: These supporting materials presented here, are not essential to the comprehension of the main paper. However, they make reference to force field parameters, supplementary mechanical behaviors, additional theoretical knowledge, and datum extracted from related literatures, as well as a list of auxiliary videos, which we believe should be useful to a subset of readers, where also included are the discussions from the reviewers of the *ACS Nano*. The readers who are interested in conducting related studies on the graphene foam(GrF)-based materials, will be welcomed to contact us.

Lists of supplementary materials:

I. Force field parameters in 3D GrF system

Table S1. Force field parameters in 3D GrF system based on 2D mesoscopic graphene model[23] and the *in-situ* SEM tests.[17]

Parameters	k_T	k_{cl}	k_φ	k_θ	ε_{ip}	ε_{op}
	r_0	r_{cl}	φ_0	θ_0	σ_{ip}	σ_{op}
Value	3720	3720	134960	933087	473	473
	25	25	90˚	180˚	23.84	23.84
Units	$kcalmol^{-1}Å^{-2}$	$kcalmol^{-1}Å^{-2}$	$kcalmol^{-1}rad^{-2}$	$kcalmol^{-1}rad^{-2}$	$kcalmol^{-1}$	$kcalmol^{-1}$
	Å	Å	—	—	Å	Å
Scope	(0,26]	(0,27]	(0˚, 180˚)	(0˚, 360˚)	(0, 50]	(0, 50]

Table S1 presents force field parameters in 3D GrF system based on the 2D mesoscopic graphene model[23] where the out-of-plane vdW interaction and the additional 3D crosslinks are both introduced based on the *in-situ* SEM tests.[17]

II. Multipeak stress–strain curve and ~45˚ ductile fracture mode

A completely different GrF sample with a length of ~99.2nm and the number of crosslinks of 830, which is filled by approximately uniform distributed flakes with the average mass density of ~471mg/cm^3, is also carried out in strain-controlled monotonic tensile loading along the vertical direction until the rupture of the numerical GrF sample. It can be seen from Figure S1 that the multipeak stress–strain curve and the ductile fracture mode near 45˚ plane from the tensile direction are both coincides well with the calculations presented in the main paper, although the ultimate strength here is larger, which is mainly from more crosslinks. The obtained effective tensile elastic modulus is equal to ~2210MPa, smaller than that of the numerical GrF sample with mass density of ~475mg/cm^3. It is necessary to point out that, due to the different volume and number of voids, the exact stress values and the number of peaks as

well as local facture details are all influenced to some degrees. However, the influence is not essential at all, as long as these influence factors still contain the real GrF features (*e.g.*, compared to the GrF flake size, the voids volume should not be much too small, otherwise the computational model can not be viewed as a GrF or GrF-base material).[S1]

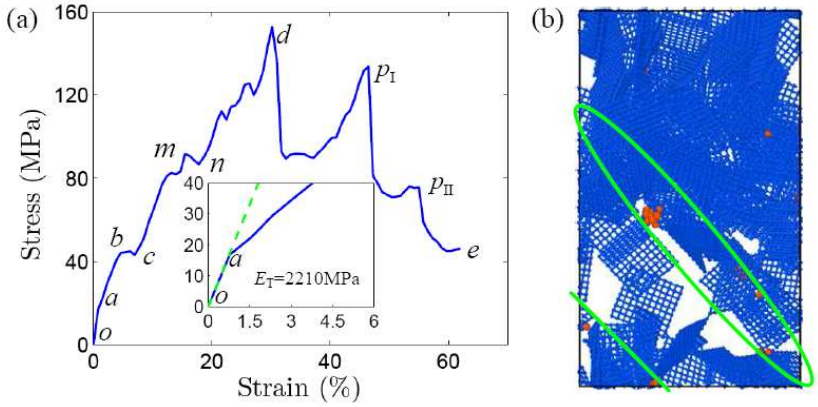

Figure S1. Uniaxial tension and fracture mode of 3D GrF with 830 linkages and the average mass density of ~471mg/cm^3. (a) Multipeak stress–strain curve in strain-controlled monotonic tensile loading based on mesoscopic graphene model. The line *oa* in the inset indicates proportional elastic line, whose slope is effective tensile elastic modulus. (b) Ductile fracture mode and the corresponding surface morphology of 3D numerical GrF. The local broken bonds near 45˚ plane from the tensile direction are highlighted by the connected red atoms and green ellipse/line.

III. Viscoelasticity and viscoelastoplasticity in the tensile deformation

To explore the pristine feature in the range of elastic stage *ob*(*o′b′*), an uniaxial loading-unloading-holding process was conducted. It can be seen clearly from Figures S2a and S2b that the elasticity of GrF is typically visco-elastic,[S2] where ~2.1% of viscous deformation is produced in loading process, and the strain during the holding with zero stress decreases to zero at 13.5ns. We also carried out a similar process to investigate the pristine feature in the hardening stage *cd* (*c′d′*), and the results are presented in Figures S2c and S2d, where ~5.1% of viscous strain is produced in the holding followed 1.8% of nonrecoverable one which is mainly from the yielding plateau. Therefore, the deformation in the hardening stage *cd* (*c′d′*) performs

a viscoelastoplasticity, and the corresponding strain recovery behavior during the holding with zero stress performs a quasi-hyperbolic behavior in typical viscoelastoplastic material.[32,S3]

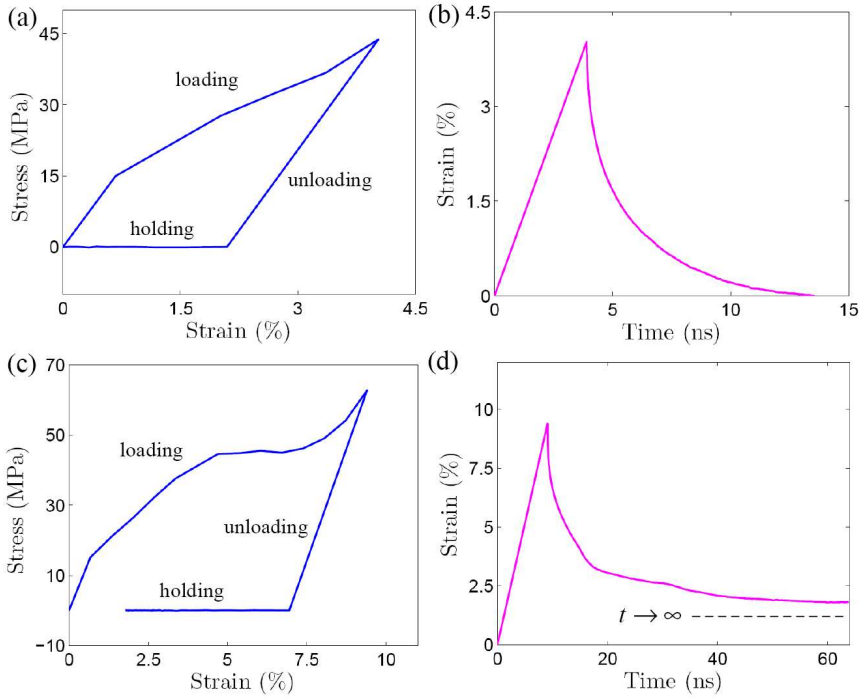

Figure S2. Viscoelasticity and viscoelastoplasticity of the GrF in the tensile deformation and strain recovery behavior. (a) Stress–strain curve in loading to 4.03% of the tensile strain, unloading to and holding at zero stress. (b) Strain–time curve without any residual strain remaining. (c) Stress–strain curve in loading to 9.4% of the tensile strain, unloading to and holding at zero stress. (d) Strain-time curve with a nonrecoverable strain of 1.8%.

Based on the experimental observations[10,17] and continuous medium mechanics theory,[35,S2] the viscoelastic part of 3D GrF should be constructed by extending/modifying the Schapery's nonlinear viscoelastic model,[32,S2] and the viscoplastic one can be, in principle, established by adopting the Ohno-Abdel-Karim's nonlinear kinematic hardening rule[S4] to describe the accumulation of irrecoverable viscoplastic strain produced during (cyclic) loading, as done by Yu *et al.*[S5] We would discuss these interesting issues in a more professional physical and/or mechanical journal in future.

IV. Tensile moduli and mass densities for different GrF-based materials

Table S2. Tensile elastic moduli and mass densities for GrF and GrF-related materials based on *in-situ* SEM tensile tests[17] and the calculating elastic moduli for different numerical GrF samples based on the mesoscopic graphene model.[23]

Authors[ref.]	Material	Density (mg/cm^3)	Modulus (MPa)
Nieto *et al.*[17]	GrF	5	0.215
Nieto *et al.*[10]	GrF-PLC	5	0.254 ± 0.0437
Xu *et al.*[18]	RGPF	71±3	270
Xu *et al.*[18]	GOPF	110±2	350
Peng *et al.*[19]	GNR-PDMS	9.33	5.7±1.1
Peng *et al.*[19]	CNT-PDMS	11.88	7.5±0.8
This study	Numerical GrF	~406	~1950
This study	Numerical GrF	~471	~2210
This study	Numerical GrF	~475	~2260
This study	Numerical GrF	~475	~2300

Table S2 presents effective tensile elastic moduli and mass densities for GrF and GrF-related materials based on *in-situ* SEM tensile tests[17] and the calculating elastic moduli for different numerical GrF samples based on the mesoscopic graphene model.[23] Note that, there are two 3D numerical GrFs with mass density of ~475mg/cm^3. The GrF with modulus of ~2300 MPa possesses 721 crosslinks, but the other with modulus of ~2260 MPa possesses 697 crosslinks.

V. Auxiliary videos for the mentioned thermodynamic processes

The following movies with AVI format, which illustrate the dynamicses at room temperature better than structural snap shots, are part of the supporting online materials:

Move1.avi represents the 3D numerical GrF sample during the tensile deformation;

Move2.avi represents the local evolution of mesostructure in 3D numerical GrF sample during the tensile deformation;

Move3.avi represents the tearing pattern of the mesoscopic graphene flake in 3D numerical GrF sample during the tensile deformation.

VI. Complementary references and notes

S1. These secondary influence factors (referring to the shape and size of the flakes, the volume and number of voids, as well as the distribution and density of linkages, *etc.*), are far from the subject of the current work, not essential to the comprehension, and are excluded for making readers concentrate on the intrinsic mechanical features of the GrF themselves. Meanwhile, as another topic, *i.e.,* the regulation of mechanics properties and behaviors, we would continue to these related issues and more in future, systematically and thoroughly.

S2. Lakes, R. *Viscoelastic Materials* (Cambridge University Press, **2009**); Christensen, R.M. *Theory of Viscoelasticity* (2^{nd}) (Dover Publications,**2010**).

S3. Jiang, H.; Zhang, J.W.; Kang, G.Z.; Xi, C.C.; Jiang, C.K.; Liu, Y.J. A Test Procedure for Separating Viscous Recovery and Accumulated Unrecoverable Deformation of Polymer under Cyclic Loading. *Polymer Testing*. **2013**, 32,1445-1451.

S4. Abdel-Karim, M.; Ohno, N. Kinematic Hardening Model Suitable for Ratcheting with Steady-State. *Int. J. Plast.* **2000**,16, 225-240.

S5. Yu, C.; Kang, G.Z.; Lu, F.C.; Zhu, Y. L.; Chen, K.J. Viscoelastic-Viscoplastic Cyclic Deformation of Polycarbonate Polymer: Experiment and Constitutive Model. *J. Appl. Mech.* **2016**, 83,041002.